PROGRESS IN AEROSPACE AND AVIATION TECHNOLOGY
e-ISSN: 2821-2924

PAAT

Vol. 5 No. 2 (2025) 58-72
https://publisher.uthm.edu.my/ojs/index.php/paat

Analysis of Flow Over Streamlined Body of High-Speed Train and Bus

Muhammad Afif Rifaie Aziz[1], Ishkrizat Taib[1]*

[1] *Department of Mechanical Engineering, Faculty of Mechanical and Manufacturing Engineering, Universiti Tun Hussein Onn Malaysia, 86400 Parit Raja, MALAYSIA*

*Corresponding Author: iszat@uthm.edu.my
DOI: https://doi.org/10.30880/paat.2025.05.02.006

Article Info

Received: 15 May 2025
Accepted: 1 November 2025
Available online: 31 December 2025

Keywords

External flow, streamlined body, pressure drags, k–ω SST model, computational fluid dynamics

Abstract

External aerodynamic flow is a key factor in determining the performance, energy efficiency, and stability of land-based vehicles such as trains and buses. Vehicles with streamlined shapes tend to experience less aerodynamic drag compared to blunt bodies, which are more prone to flow separation and larger wake regions. This study aims to investigate and compare the external flow behavior over a streamlined body and a blunt body using Computational Fluid Dynamics (CFD). The objective is to understand how shape influences boundary layer development, flow separation, wake formation, and overall drag characteristics. Two geometries are modeled: a high-speed train, representing the streamlined body, and a bus, representing the blunt body. The train model is scaled to a width of 0.3 m, height of 0.4 m, and length of 3.2 m, while the bus model has a width of 0.244 m, height of 0.37 m, and length of 1.127 m. The flow inlet is being compared under incompressible conditions at air flow speeds of 10 m/s, 20 m/s, and 30 m/s through the opening, using three different values. For an accurate representation of wall boundary layers, a mesh is organized with fewer elements near walls, and the k-ω model of turbulence is used. To see how the external flow works over every geometry, both velocity contours and pressure distributions are evaluated. It is shown that the train's reduced geometric dimensions lead to less detached flow and a tighter wake, which then causes less drag. Conversely, the basic design of buses causes the flow to divide earlier and spread, which allows for more resistance. The results indicate that body shape has a big impact on airflow and support using streamlined designs for higher aerodynamic performance in vehicles.

1. Introduction

The aerodynamic behavior of land-based vehicles has long been recognized as a significant factor influencing fuel efficiency, stability, and environmental performance. In the transportation industry, especially for vehicles operating at moderate to high speeds such as buses and trains, aerodynamic drag accounts for a substantial portion of the total resistance experienced during motion [1]. As global efforts intensify toward energy conservation and emissions reduction, optimizing vehicle design for better aerodynamic performance has become a key engineering objective. One of the most effective strategies for reducing aerodynamic drag is implementing streamlined body shapes that guide airflow smoothly around the vehicle and minimize disturbances leading to energy loss, as discussed by several authors [2], [3].

The streamlined form includes steady bends, narrower faces, and longer back ends, which allow for less flow separation and less creation of big wakes [4]. In contrast, vehicles with blunt shapes do not cause any useful effects

since they produce flow separation right away, strong turbulent zones behind them, and lots of pressure drag [5]. Many designs used on buses are simple because of manufacturing difficulties, space issues, and expenses. Nevertheless, using these shapes increases fuel use and makes it harder to keep the aircraft steady and fast when facing strong side winds or going at top speeds [6], [7]. The current study addresses this practical challenge by comparing the external flow behavior over a streamlined body and a blunt body using Computational Fluid Dynamics (CFD). The aim is to evaluate how differences in body shape affect boundary layer development, flow separation, wake formation, and aerodynamic drag, with the ultimate goal of informing future vehicle design improvements. This comparison is particularly relevant as it allows for the identification of key aerodynamic advantages associated with streamlined geometries by several authors [8]-[10].

In CFD, the flow field is resolved by numerically solving the fundamental governing equations—the continuity and Navier–Stokes equations using the finite volume method. These equations account for mass and momentum conservation and are solved iteratively across a discretized computational domain that replicates the geometry of the actual system. To model turbulence, which introduces a wide range of fluctuating scales, suitable turbulence models must be employed. Among the various models available, the Reynolds-Averaged Navier–Stokes (RANS) approaches—such as the standard k–ε, realizable k–ε, RNG k–ε, and k–ω SST models are widely used due to their computational efficiency and adequate accuracy for steady-state simulations [11]-[13]. Despite the superior resolution of transient turbulent structures provided by Large Eddy Simulation (LES) methods, their high computational demands generally restrict their use to research applications. Therefore, this study employs the k–ω SST model, which effectively captures flow separation and swirl effects common in geometries with internal obstacles.

Simulations are run with ANSYS Fluent in a stable and incompressible condition to perform the analysis. The impact of velocity on aerodynamic behavior is observed by testing at inlet velocities of 10 m/s, 20 m/s, and 30 m/s. A fine mesh around the walls is used on a regular structure to model shear, pressure differences, and wake development accurately. The k-ω turbulence model is chosen because it is suitable for capturing near-wall flow and separations in external flow settings [14]. Furthermore, as the inlet velocity increases from 10 m/s to 30 m/s, the aerodynamic deficiencies of the blunt body become even more pronounced. Higher flow speeds amplify the turbulent wake and pressure losses in the blunt geometry, while the streamlined train continues to exhibit stable, attached flow with manageable drag levels. This highlights the robustness of streamlined shapes in coping with a wide range of operating speeds [15], [16].

Simulation studies covered two kinds of transport: a streamlined high-speed train and a blunt bus. Recent research on flow for streamlined trains was used to ensure the geometry of the high-speed train is accurate. The model is 0.3 meters wide, 0.4 meters high, and 3.2 meters long. But for the bus model, the builder divides down real-world sizes by a factor of 0.25, making its width 0.244 m, its height 0.37 m, and its length 1.127 m. The purpose of these scaled models is to permit accurate evaluation under controlled environments without losing the geometry of the original objects [17].

The results of the simulation point out noticeable differences in how the two models perform in the air. The train shows a well-fitted flow that separates little, and its wake is largely narrow, leading to significantly reduced pressure drag. Alternatively, the simple bus geometry causes flow to detach early on, leading to a bigger separated region and larger wake on the bus, all of which raise its overall drag force. The use of velocity and pressure contours, as well as wake depictions, confirms these results [18], [19].

The CFD simulations conducted in this study strongly reinforce the aerodynamic superiority of streamlined vehicle designs. The high-speed train model, with its gradual curvature and tapered profile, effectively manages airflow, reduces drag, and minimizes flow disturbances [20]. In contrast, the blunt bus design suffers from flow separation and significant pressure loss, resulting in higher aerodynamic drag. These findings are relevant for the transportation industry, especially in urban and high-speed travel sectors, where fuel efficiency and stability are paramount. The insights gained from this study can support informed decision-making in vehicle design, promote the adoption of aerodynamically optimized shapes, and contribute to the development of more sustainable and energy-efficient transportation systems. Additionally, the use of CFD as a predictive and diagnostic tool is reaffirmed, offering a powerful, non-invasive, and cost-effective method for evaluating and improving aerodynamic performance in future vehicle development projects.

2. Methodology

This study investigates the external aerodynamic flow behavior around two distinct vehicle geometries: a high-speed train representing a streamlined body and a bus representing a blunt body. The objective is to analyze how differences in shape affect flow features such as velocity distribution, pressure variation, wake formation, and flow separation under different flow conditions. The simulations are carried out using Computational Fluid Dynamics (CFD) techniques, which allow for detailed examination of complex fluid behavior around external surfaces without the need for physical prototypes.

Progress in Aerospace and Aviation Technology Vol. 5 No. 2 (2025) p. 58-72

2.1 Geometry of The High-Speed Train and Bus

In this study, two distinct vehicle geometries are selected to represent contrasting aerodynamic profiles: a high-speed train as the streamlined body and a bus as the blunt body. The high-speed train geometry is scaled down to 0.3 m in width, 0.4 m in height, and 3.2 m in length while preserving its aspect ratio. In contrast, the bus geometry, developed by proportionally scaling down real-world dimensions to 0.244 m in width, 0.37 m in height, and 1.127 m in length, represents a typical blunt-shaped public transport vehicle with a vertical front, sharp edges, and a flat rear. These characteristics are known to induce early flow separation and generate large wake regions. Both geometries are created using CAD software and placed in identical computational domains to ensure consistent boundary conditions. This setup enables a direct comparison of how shape influences key aerodynamic phenomena such as flow attachment, wake formation, and pressure drag. Figs. 1 and 2 show the geometry of the high-speed train and bus complete with subtracted features from the simulation box to create a fluid domain.

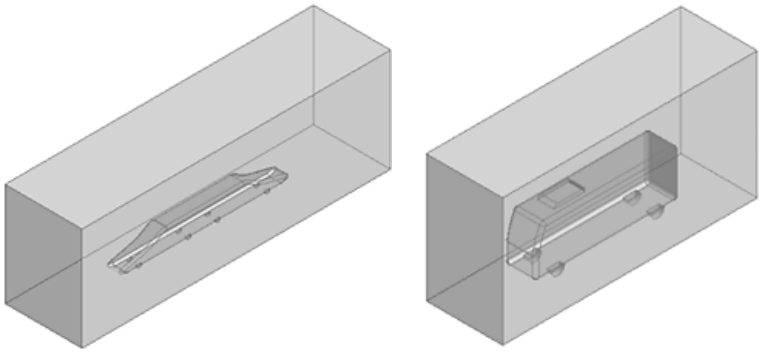

(a) **(b)**

Fig. 1 *Geometry box view (a) High-speed train; (b) Bus*

(a) **(b)**

Fig. 2 *Geometry front view (a) High-speed train; (b) Bus*

2.2 Meshing

The accuracy, stability, and productivity of the simulation depend on the quality of the mesh. This study uses ANSYS Mesh for meshing, a dependable system that produces effective grids for complex external flow simulations. The use of a tetrahedral mesh is justified by the shape of the models since it can manage the challenging surfaces and corners found on the streamlined high-speed train and the blunt-edged bus. This meshing strategy provides a balanced compromise between computational cost and the required level of detail necessary to resolve key aerodynamic features. For the high-speed train model (Geometry 1), the default element size is set at 325 mm, yielding a total of 94785 nodes. For the bus model (Geometry 2), the element size is 115.76 mm with a total of 72147 nodes. These configurations are chosen to ensure consistent resolution across both geometries while keeping the mesh complexity manageable. With the mesh in place, flow separation, wake formation, and pressure changes can be accurately handled in areas of fast-moving fluid. Fig. 3 represents the mesh for Geometry 1 and Geometry 2, indicating the areas of surface discretization and refinement. This approach is proven valid through a mesh independence study, showing that no further improvement of the mesh greatly changes the results.

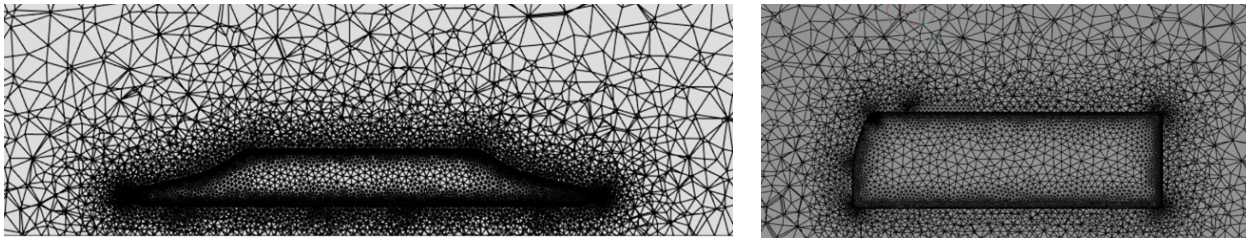

(a) (b)

Fig. 3 *Meshing of vehicle geometry (a) High-speed train; (b) Bus at default setting*

2.3 Governing Equation

The governing equations for the simulation of turbulent flow in this study are based on the fundamental equations of fluid dynamics, such as continuity (Eq. (1)) and Navier–Stokes (Eq. (2)). The domain involving obstacles that produce complex flow patterns requires these equations to describe the physical behavior of fluid flow. The continuity equation ensures the conservation of mass. It also says the rate at which mass enters a control volume equals the rate at which it leaves if there are no sources or sinks. For incompressible flow, fluid density is constant, and this is an important principle.

On the other hand, the Navier–Stokes equations describe the time rate of change of the three momentum components of the fluid. They account for the effects of pressure, viscous forces, and body forces acting on the fluid. These equations are vectors and are time dependent, thus modelling the steady and unsteady flow behavior. In the turbulent regime, they become increasingly more complex because fluctuating velocity components are present and must be modeled with turbulence closure techniques. These equations, when taken together, represent the basis for the accurate description of fluid motion under a great variety of conditions, and this study solves them numerically in this form using the finite volume method in ANSYS Fluent.

$$\frac{\partial \rho}{\partial t} + \nabla \cdot (\rho \vec{v}) = 0 \tag{1}$$

$$\rho \left(\frac{\partial \vec{v}}{\partial t} + \vec{v} \cdot \nabla \vec{v} \right) = -\nabla p + \mu \nabla^2 \vec{v} + \vec{F} \tag{2}$$

where ρ is fluid density, p is pressure, $\vec{v}$ is the velocity vector, μ is dynamic viscosity, and $\vec{F}$ represents body forces.

Using the SST formulation of the k–ω turbulence model, ANSYS Fluent is employed to model external turbulent flow properly around the high-speed train and bus geometries. The blending function in this model ensures it works well in predicting flow separation, adverse pressure gradients, and wake formation, key points in this simulation. A pressure-based solver, using the SIMPLE algorithm for coupling pressure and velocity, addresses steady-state, incompressible, and turbulent flow situations. The stable and accurate second-order upwind discretization method is applied to every governing equation. With this configuration, accurate predictions of aerodynamic responses can be made for both streamlined and blunt vehicles as velocity changes.

2.4 Boundary Condition and Parameter Assumption

Given the same boundary conditions and assumptions for all simulation cases, the external flow around the high-speed train and bus geometries was simulated under three different inlet velocities: 10 m/s, 20 m/s, and 30 m/s. A uniform velocity inlet boundary condition is applied at the front face of the computational domain, ensuring consistent flow across all cases. The pressure outlet boundary condition is set at the rear face with a gauge pressure of 0 Pa, allowing the airflow to exit the domain freely while maintaining numerical stability. The surfaces of both vehicle geometries and the outer walls of the domain are treated as no-slip walls to account for viscous effects and accurately capture boundary layer formation. This setup enables the model to resolve key aerodynamic features such as flow separation, wake development, and wall-bounded turbulence. The regions for each boundary condition inlet, outlet, and wall surface are clearly defined during the preprocessing phase to ensure consistency across all simulation scenarios. A schematic representation of these boundary regions is shown in Fig. 4, while the surface of the geometry is shown in Fig. 5 by using a section plane.

A working fluid of liquid water is selected from the standard Fluent material database. It is assumed that the density and viscosity of the fluid throughout the domain are constant. The internal obstacles are assumed to be stationary with no slip condition (the fluid's velocity at the boundary is zero). This assumption is realistic for the viscous behavior of air when it interacts with solid surfaces. The pressure-velocity coupling is accomplished by

Progress in Aerospace and Aviation Technology Vol. 5 No. 2 (2025) p. 58-72

using the SIMPLE (Semi-Implicit Method for Pressure-Linked Equations) algorithm for the solution method. The iterative method is generally used in incompressible flow problems to obtain a convergent and a stable numerical solution.

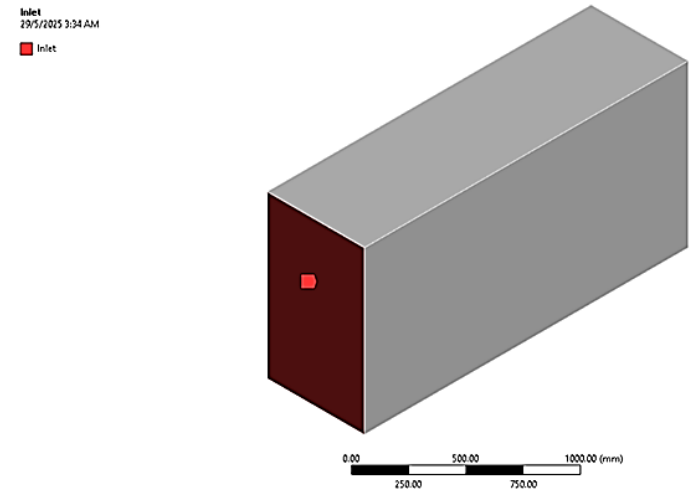

(a)

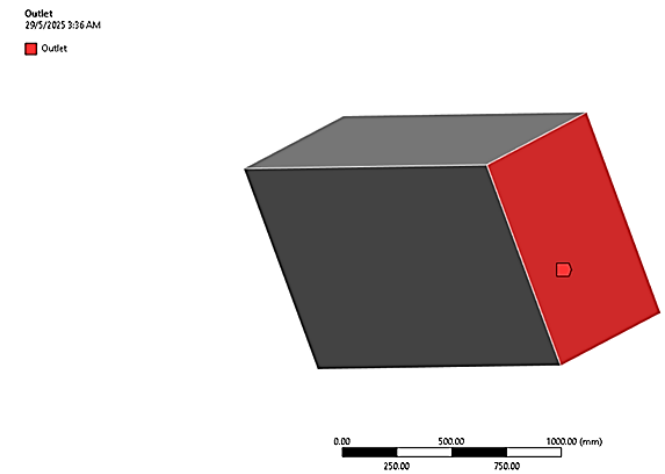

(b)

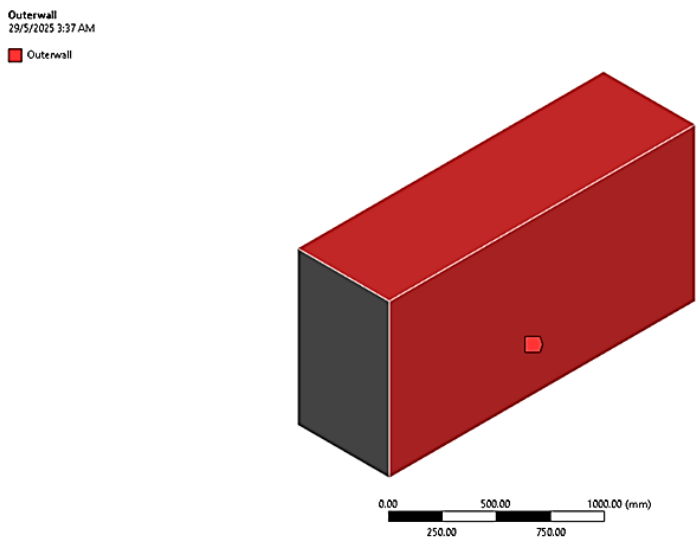

(c)

Fig. 4 *Named selection (a) Inlet; (b) Outlet; (c) Outerwall*

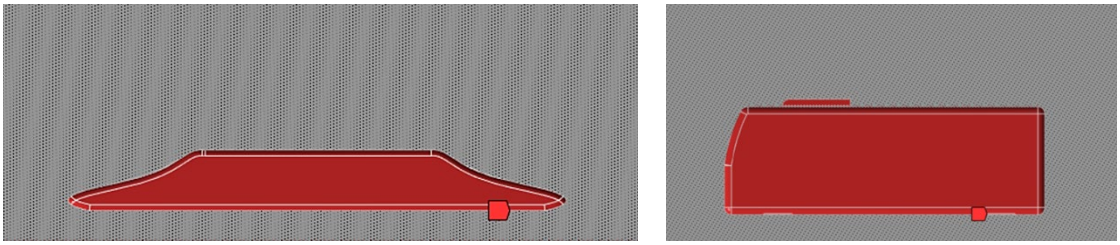

(a) (b)

Fig. 5 *Inner surface (a) High-speed train; (b) Bus*

2.5 Analysis

The main objective of the post-processing and analysis phase is to assess the external aerodynamics of a high-speed train (with a streamlined body) and a bus (with a blunt body) as they travel at steady-state turbulent conditions and different inlet speeds. To find out how a body's form affects its ability to flow through the air, it's important to look at boundary layer growth, flow separation, wake formations, and orientation of drag and lift forces, among other factors. A key part of the analysis is how the boundary layer grows on each vehicle. Examining velocity and the flow field close to the surfaces shows the thickness and speed of the boundary layer as air flows over the front, top, and rear parts of the wing. The layer of fluid adheres closely to the train's surface and remains thin in the streamlined lines, resulting in low air resistance. Unlike cars, the bus's simple, rectangular shape results in more thickness in the bounding air layers and causes separation and turbulence to develop sooner at the back corners.

Velocity vector plots and streamline plots help to find the separation points in fluid flow. The plots make it obvious where detachment of the airflow takes place. As the high-speed train's speed increases, separation begins to happen gradually, since its rear end blends into the shape of the track more smoothly toward the tail end. Furthermore, the rear portions of the bus's vertical face experience sudden and quick separation. This causes important areas of high recirculation and a less stable airflow. Formation of wakes after the ship passes through the water is a key factor to consider. Using streamlines and velocity contour plots helps find out the shape, dimensions, and vigor of the wake produced by every vehicle. The train's wake is narrow and even and has less disturbance, while the bus's wake covers a greater area, is unpredictable, and has high variations in airspeed, as well as vortexes. This is because pressure drag depends on the surface pressure, and this is determined by reviewing the surface pressure and finding the pressure coefficient (Cp) of the body.

Other than pressure, the aerodynamic drag force and, where appropriate, the lift force applied to each high-speed train and bus are considered as well. Pressure and shear stresses are integrated all over the surfaces of the models to attain these values. Because of fewer pressure differences, the train's attached flow, and a smoother shape, it experiences much less drag. Though lift forces are not the main factor considered in ground vehicles, they are still looked at, especially to detect any impacts on the vehicle's vertical motion caused by streamlining or air flow beneath it. The analysis employed numerical data and visual aids to determine the impact of streamlined or blunt shapes on aerodynamic efficiency. The way the boundary layer works, separation points occur, wakes evolve, and forces develop are all important signs of how the external flow responds to the shape of the body.

3. Results and Discussion

To evaluate the aerodynamic performance of different vehicle shapes, this study compares two geometries: Geometry 1, representing a streamlined high-speed train, and Geometry 2, representing a blunt urban bus. The scaled dimensions of the train are 0.3 m in width, 0.4 m in height, and 3.2 m in length, while the bus measures 0.244 m in width, 0.37 m in height, and 1.127 m in length. These geometries are subjected to external turbulent flow at three inlet velocities: 10 m/s, 20 m/s, and 30 m/s. All simulations are performed under identical boundary conditions to ensure a consistent basis for comparison. The objective is to investigate how vehicle shape and flow velocity influence key aerodynamic characteristics. Specifically, the analysis focuses on (i) boundary layer development, (ii) flow separation points, (iii) wake formation and pressure drag, and (iv) drag coefficient and drag forces acting on the vehicle bodies. By comparing results between the streamlined and blunt geometries across different flow velocities, the study aims to identify how shape optimization can improve flow behavior, reduce aerodynamic drag, and enhance vehicle efficiency in practical applications.

Progress in Aerospace and Aviation Technology Vol. 5 No. 2 (2025) p. 58-72

3.1 Boundary Layer Development

The main feature of turbulent external flow is the way the boundary layer changes and grows along the surface of the body. How thick the boundary layer is, how it grows, and whether it separates depend a lot on the object's shape and the air speed passing by it. This study looks in detail at how the boundary layer forms on a streamlined high-speed train and a blunt-shaped bus. Making the comparison clarifies the role of surface shape in the flow within the boundary layer. Because the high-speed train has a smooth and slender shape, it remains in attached flow on most of its surface regardless of the inlet velocity. Alternatively, the angular nature of the bus reduces the airspeed, especially at those places with sharp corners, causing the layer of air near the rear to detach much earlier and be thicker. The two patterns become easier to see when the inlet velocity grows higher. In Fig. 6, we can see the boundary layer around the train. Fig. 7 shows this same thing happening to the bus when the vehicle travels at 10 m/s, 20 m/s, or 30 m/s.

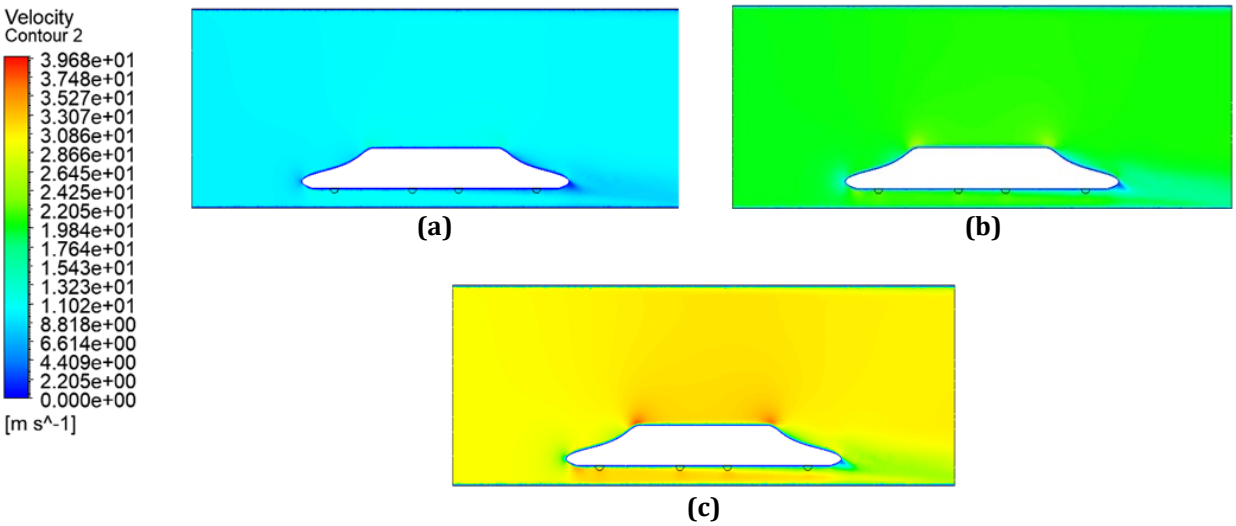

Fig. 6 *Velocity contour of high-speed train (a) 10 m/s; (b) 20 m/s; (c) 30 m/s*

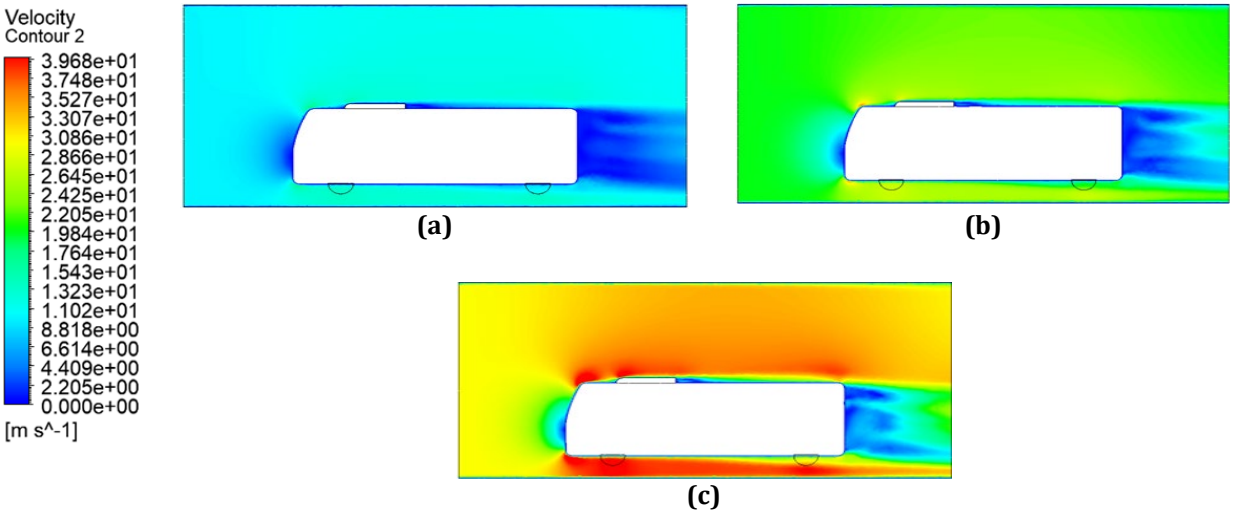

Fig. 7 *Velocity contour of bus (a) 10 m/s; (b) 20 m/s; (c) 30 m/s*

When the vehicle moves at 10 m/s, the thin boundary layer is attached to most of the bus, but small parts of it do separate near the end. As velocity rises to 20 m/s, the train's boundary begins to grow far outward yet stays linked all along its front part. At the same time, the bus has a thicker boundary layer, and small separation bubbles appear close to its rear. A smooth blunt bus becomes increasingly unstable as its speed rises to 30 m/s, which makes the boundary layer split earlier, leads to a thicker wake, and brings about more pressure drag. Trains have a better aerodynamic design, so air flows through them nearly without flaps or splitting. The front of the bus is narrow, and the rear is flat, which leads to an unfavorable change in pressure that makes the boundary layer detach at a lower speed. Meanwhile, the train's rounded nose and slim tail reduce obstruction to air, which results in thinner air layers and better attachment over the vehicle when moving at higher velocities. These actions

indicate that sleeker bodies help keep division from happening early and make it simpler to manage the boundary layer during high turbulence.

Figs. 6 and 7 also use velocity contour plots to illustrate the growth of the boundary layer. They emphasize the area close to the wall where the flow speed goes from zero to the mainstream speed. Changes in the thickness of the velocity gradient can show the position of the boundary layer along the surfaces of these shapes. When the bus is moving at 30 m/s, the boundary layer thickens and changes into a separated zone, yet the train shows smoother changes and less steep gradients in the near-wall area. In conclusion, both body shape and flow speed strongly influence the growth of the boundary layer. High-speed trains have thinner and less unstable boundary layers, whereas buses with large front shapes make the layers detach faster and grow bigger. As a result, these factors influence the roll-up process in an airplane's wake, the pressure exerted on the plane, and its overall efficiency, which will be explored in detail next.

3.2 Flow Separation Point

Flow separation occurs when the boundary layer can no longer overcome the adverse pressure gradient along a surface, leading to flow detachment and the formation of low-pressure recirculation zones. Both the body's geometry and the inlet flow velocity closely influence this phenomenon. Figs. 8 and 9 show the flow separation that occurs for both geometries, which are the high-speed train and bus, at different inlet velocities.

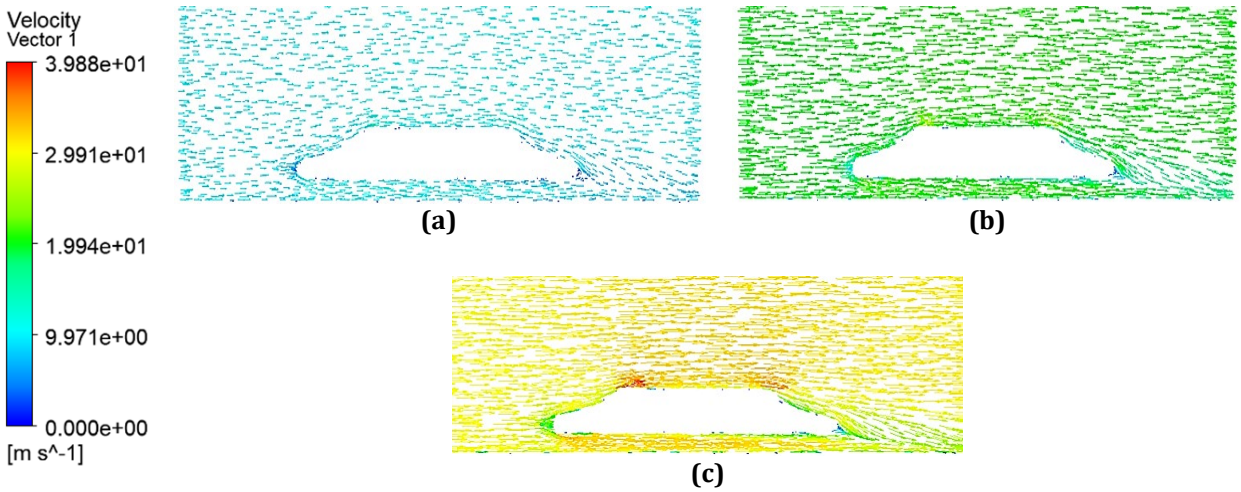

Fig. 8 *Velocity vector for high-speed train (a) 10 m/s; (b) 20 m/s; (c) 30 m/s*

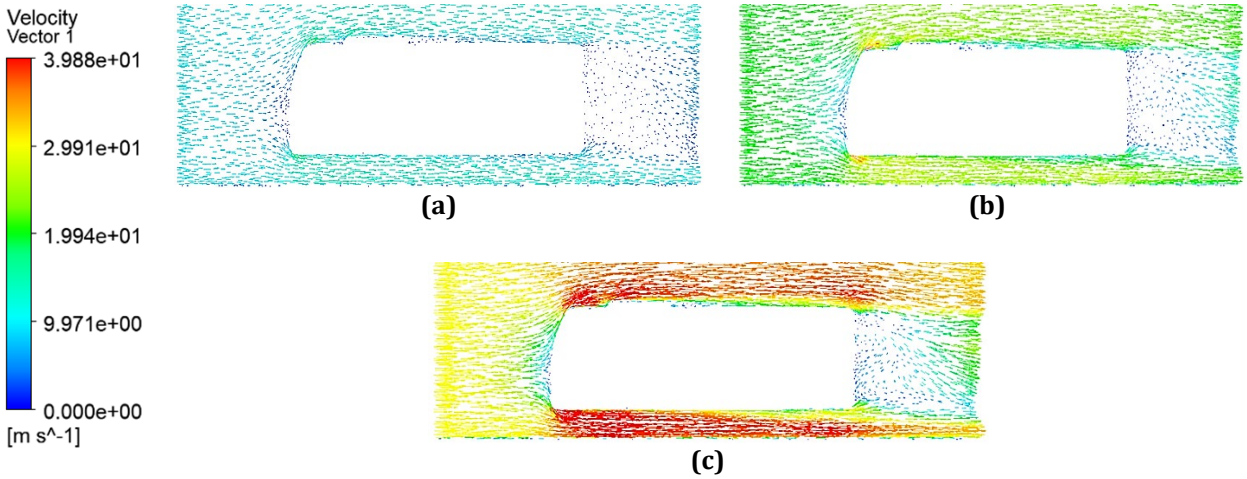

Fig. 9 *Velocity vector for bus (a) 10 m/s; (b) 20 m/s; (c) 30 m/s*

Blunt bus geometry in this study separates the flow rapidly and strongly because its sharp corners and vertical back surface promote the formation of strong adverse pressure. When the vehicle's speed increases from 10 m/s to 30 m/s, the point of air separation along the side of the bus moves forward, allowing more air to enter the wake region behind the vehicle. At very high velocities, widely separated areas and vortices become the main features in the wake, which results in considerable aerodynamic resistance. In addition, the streamlined high-

Progress in Aerospace and Aviation Technology Vol. 5 No. 2 (2025) p. 58-72

speed train keeps the air attached over most of its body because of its slowly tapering front and rear. If flow separation does occur, it happens much further ahead and is not as serious as the previous problem. Even as speed reaches 30 m/s, the region where the flow separates is still slim and equal on the top and bottom, which means the flow is well-guided and the pressure drag is lower.

3.3 Wake Formation and Pressure Drag

Wake formation is a key indicator of aerodynamic efficiency, as it directly relates to flow separation and pressure drag. In external flows, the wake is the low-pressure, turbulent region formed behind a body where the flow detaches. The geometry of the object and the flow velocity heavily influence the shape and size of this wake. Figs. 10 and 11 show the wake formation occurring at both geometries at different inlet velocities. At all simulated speeds, the flat front of the bus causes a big, skewed wake. Because the vehicle's back surface is vertical and the leading edges are not rounded, there is a sudden split in the airflow that results in a wide area of slow-moving air behind the vehicle. When the inlet speed goes from 10 m/s to 30 m/s, the wake becomes more unstable, and there is a stronger shedding of vortices and increased turbulence. Since the wake area grows a great deal in the back, the pressure changes from the front door to the rear of the bus strongly, increasing the bus's resistance.

Alternatively, the small profile of streamlined trains leads to a stable and narrow wake when moving at speeds less than those of conventional vehicles. The sleek form significantly reduces the speed and size of the rear area. The truck's airflow is more symmetrical than the bus's, even as the truck speeds up in the simulation. The way the pressure drops along the train body points to less form drag and a better-functioning reattachment of airflow. The contour plot and streamline images (Figs. 10 and 11) illustrate the wake features and their shape for both configurations. As is evident from these results, aerodynamically shaped bottoms minimize wake creation, whereas blunt bottoms worsen it, which causes increased losses from pressure forces. This points to the need for wake control to better the vehicle's aerodynamics and drop drag forces.

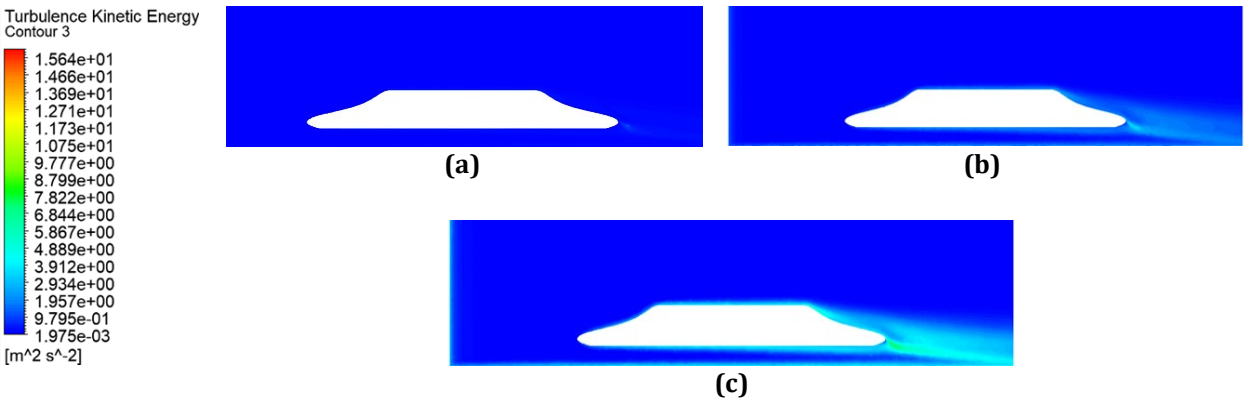

Fig. 10 *Turbulent kinetic energy contour of high-speed train (a) 10 m/s; (b) 20 m/s; (c) 30 m/s*

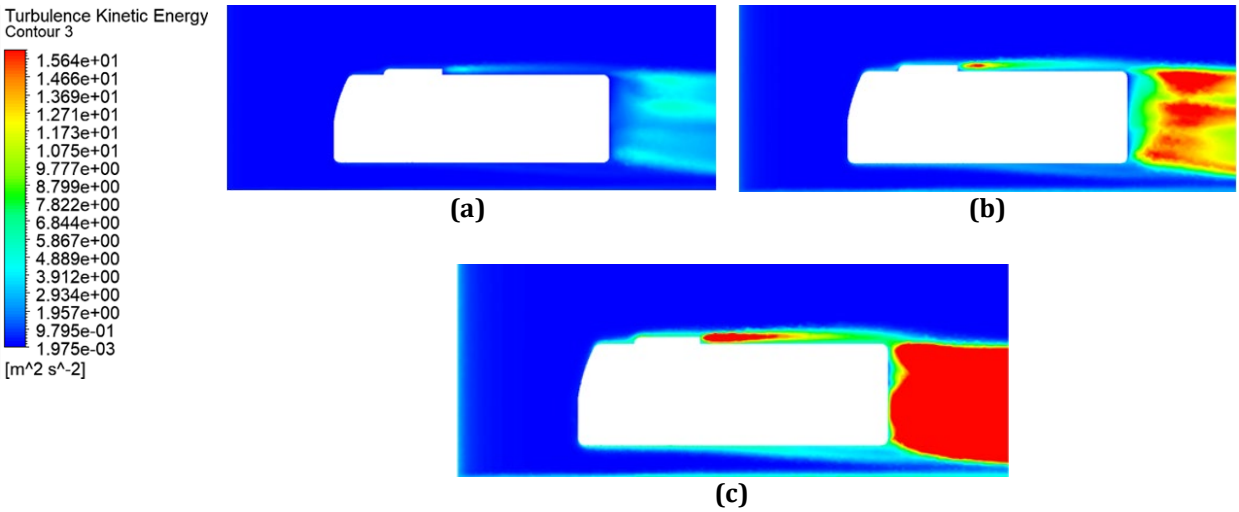

Fig. 11 *Turbulent kinetic energy contour of bus (a) 10 m/s; (b) 20 m/s; (c) 30 m/s*

3.4 Drag Force and Drag Coefficient

Pressure drag is a major component of total aerodynamic drag, especially in external flows dominated by flow separation and wake formation. It arises due to the pressure differential between the front and rear surfaces of a body and is highly sensitive to shape and flow velocity. This study uses ANSYS Fluent to find the pressure drag and drag coefficient values for both the high-speed train (with a streamlined shape) and the bus (with a blunt shape) at speeds of 10 m/s, 20 m/s, and 30 m/s. The results present a clear picture of the aerodynamic performance of each configuration. Tables 1 and 2 below show the data of the pressure drag and drag coefficient for both geometries at different inlet velocities.

The shape of the train helps avoid large pressure drag at any speed by stopping the flow from separating and allowing it to attach again smoothly. With an increased inlet velocity, pressure drag for the train goes up from 0.01132 N to 0.08310 N, while the value of its drag coefficient increases from 0.000185 to 0.001357. Such an increase is normally how streamlined bodies work, so drag levels remain the same and reliable even as speed increases. However, because buses are long and wide, their figures create much more pressure drag compared to cars. Drag is equal to 0.45283 N if the vehicle travels at 10 m/s and 1.40066 N when it travels at 30 m/s. The related drag coefficients become bigger and reach their highest point of 0.022868 at the top speed. Because Cd is so high, the back of the bus experiences strong separation of air, building a big wake and resulting in substantial loss of power.

Table 1 *Data of drag pressure and drag coefficient for high-speed train*

Inlet velocity (m/s)	Drag pressure (N)	Drag coefficient
10	0.01132	0.000185
20	0.04063	0.000663
30	0.08310	0.001357

Table 2 *Data of drag pressure and drag coefficient for bus*

Inlet velocity (m/s)	Drag pressure (N)	Drag coefficient
10	0.45283	0.007393
20	1.00882	0.016472
30	1.40066	0.022868

3.5 Pressure on the Vehicle Surface

Surface pressure distribution is a key factor in understanding aerodynamic performance, as it directly influences pressure drag and overall flow behavior around a body. In this study, surface pressure contours are used to examine how the shape of the high-speed train and bus geometries affect the distribution of pressure across their surfaces at inlet velocities of 10 m/s, 20 m/s, and 30 m/s. Figs. 12 and 13 show the pressure contour for both geometries at different inlet velocities.

On a streamlined high-speed train, the pressure is highest at the nose (stagnation point) and little by little decreases while the train speeds up smoothly. Pressure gradually recovers at the back of the aircraft, making the inside pressure nearly flat. The longer geometry helps maintain smooth airflow, which gradually builds up pressure and reduces air turbulence. The pressure plots are symmetric across the middle line, which demonstrates the flow is quite steady regardless of the speed the vehicle reaches. But the boxy design of the bus shows clear differences in pressure. The air directly strikes the object's front face, creating high pressure there.

After the front part of the airplane reaches stagnation, its rear part undergoes early flow separation because of the sharp turns and vertical area at the back. There is a large and enduring low-pressure region at the rear, which shows a wide wake zone behind the aircraft. Because of this, there is a larger pressure difference between the front and back of the bus, which leads to higher drag. The pressure contour plots clearly highlight these differences. While the bus surface experiences a violent rise and fall in pressure, and waves break off along its surface, the train remains up and down in a much smoother manner. As a result, we can confirm that the early drag analysis was sound and streamlined forms offer a better ability to ensure balanced pressure on the vehicle.

Progress in Aerospace and Aviation Technology Vol. 5 No. 2 (2025) p. 58-72

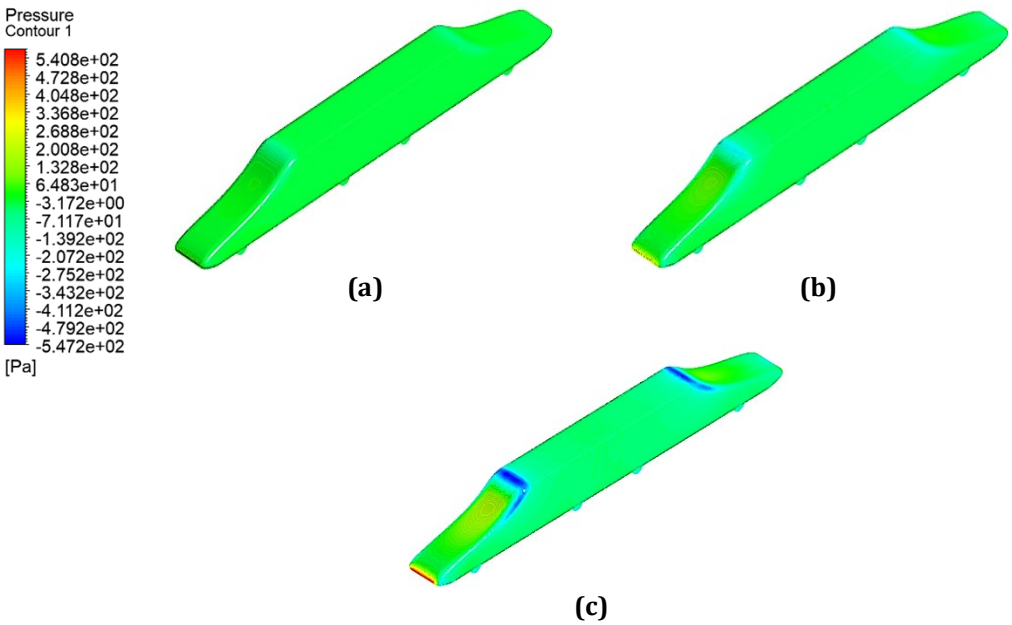

Fig. 12 *Pressure contour on high-speed train surface (a) 10 m/s; (b) 20 m/s; (c) 30 m/s*

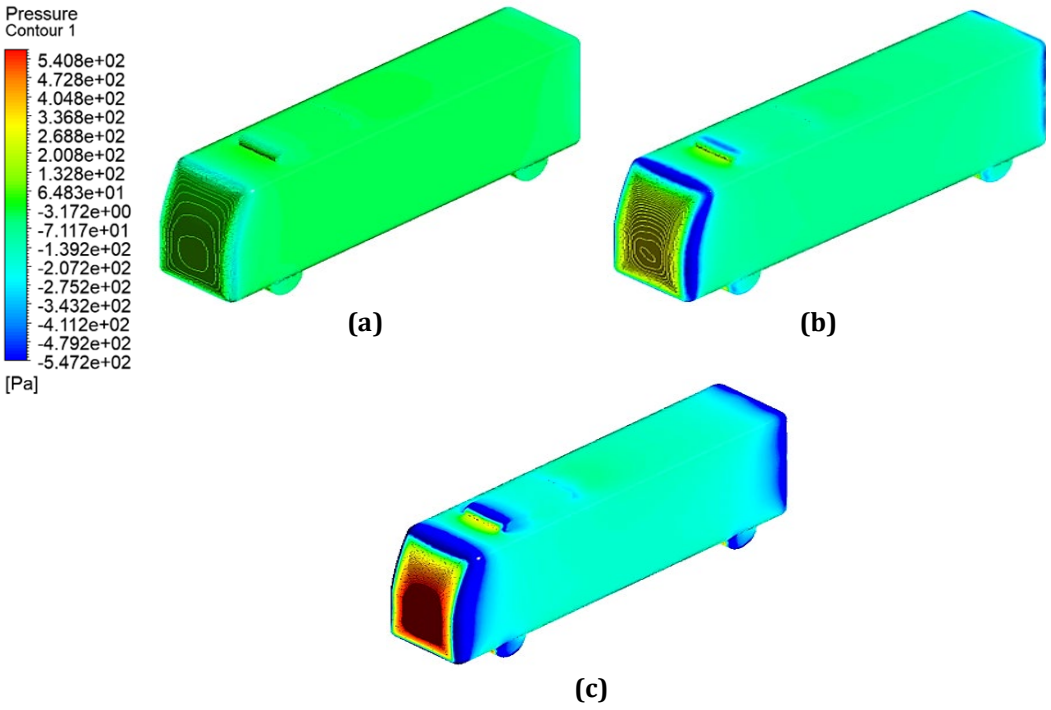

Fig. 13 *Pressure contour on high-speed train surface (a) 10 m/s; (b) 20 m/s; (c) 30 m/s*

3.6 Grid Independent Test

To ensure that the mesh resolution does not significantly affect the accuracy of the CFD results, a Grid Independence Test (GIT) is performed separately for each geometry. This test is essential for validating the reliability of the numerical solution and for determining an optimal mesh size that balances accuracy with computational efficiency.

For Geometry 1 (the high-speed train), five mesh configurations with varying element sizes are tested under identical boundary and flow conditions. Convergence is ensured in each case before progressing to the next. The velocity distribution and pressure drop are monitored and compared across mesh levels. The solution is considered grid-independent when successive mesh refinements lead to negligible changes in key flow parameters. Based on the test results, a tetrahedral mesh with an element size of 30 mm, corresponding to 348819 nodes, is selected for its high accuracy and manageable computational cost.

For Geometry 2 (the bus), the same testing procedure is applied. Multiple mesh sizes are analyzed under the same simulation settings. The optimal mesh is found to be one with 12 mm element size and 341569 nodes, which provides sufficiently detailed flow resolution without excessive computation time. Fig. 14 below shows a close-up of the meshing for Geometry 1 and Geometry 2, highlighting the best mesh selection determined through the grid-independent test.

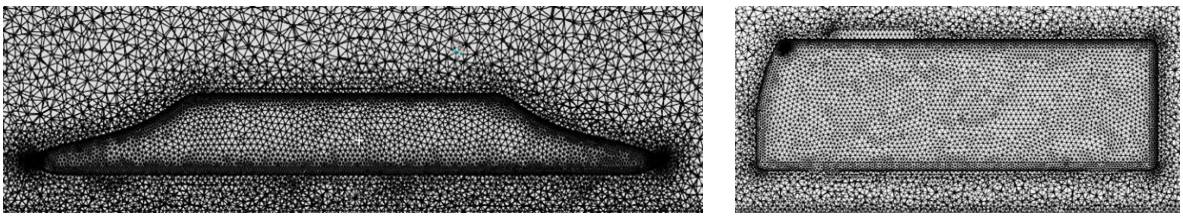

(a) **(b)**

Fig. 14 *(a) Geometry 1; (b) Geometry 2*

To verify the mesh independence, velocity magnitude along the Z-axis is plotted and compared for different mesh densities. The plots show minimal variation between the last two mesh refinements, confirming that the solutions have converged and are mesh independent. Fig. 15 illustrates the comparison graph, highlighting the negligible differences in velocity profiles and validating the adequacy of the selected meshes for final simulations. The GIT chart for both geometries doesn't include the default meshing. Tables 3 and 4 show the summary of different element sizes for both geometries.

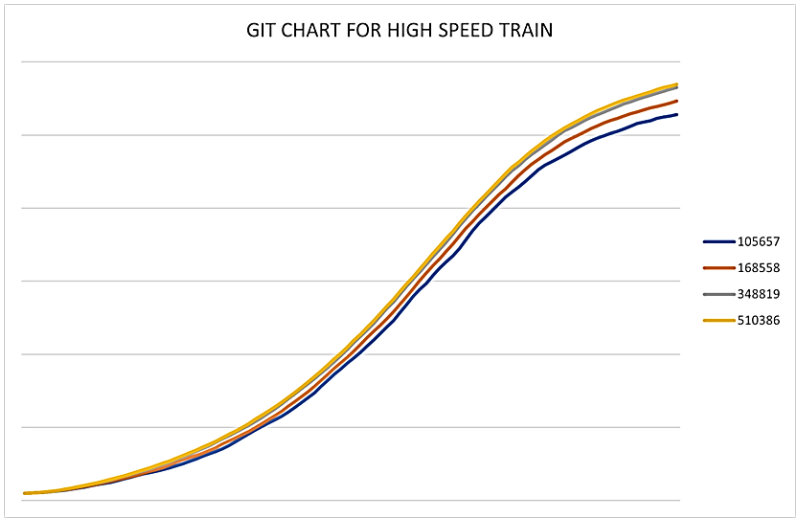

(a)

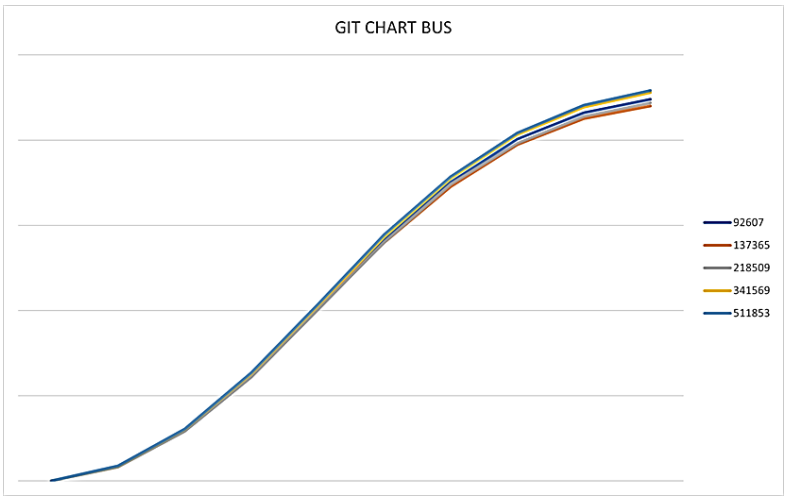

(b)

Fig. 15 *(a) GIT chart for high-speed train; (b) GIT chart for bus*

Progress in Aerospace and Aviation Technology Vol. 5 No. 2 (2025) p. 58-72

Table 3 *Summary of different element size meshes for Geometry 1 (high-speed train)*

Element size (mm)	Nodes	Elements
Default (325.00)	94785	520849
100	105657	574439
50	168558	908771
30	348819	1878139
25	510386	2771407

Table 4 *Summary of different element size meshes for Geometry 2 (bus)*

Element size (mm)	Nodes	Elements
Default (115.76)	72147	391601
30	92607	492667
20	137365	727443
15	218509	1163094
12	341569	1830647
10	511853	2767518

3.7 Comparison with Published Values

Comparisons were performed of the CFD results for external flow over both smooth (high-speed train) and blunt (bus) objects and published values from peer reviews. The simulations were performed with the k–ω SST turbulence model to confirm aerodynamic results at inlet velocities set at 10, 20, and 30 meters per second. The high-speed train ran successfully, displaying aerodynamic benefits by facing virtually no separation, having a narrower flow behind it, and producing less drag from the air. On the other hand, the blunt bus started showing flow detachment early, formed a big, separated flow area, and had higher total drag forces. These observations align with the existing research. Xuan et al. [1] reported that bodies with simple, streamlined shapes reduce drag, particularly at elevated speeds. Zhang *et al.* [4] pointed out that making the car's back curved and tapered decreases the flow separation and wake formation, as the CFD study on the train also indicated. Furthermore, Abdolahipour *et al.* [5] proved that vehicles with straight fronts and sharp sides have immediate separation and create a large turbulent wake, as was seen in the bus case. Halfina *et al.* [14] have confirmed that the k–ω SST model is accurate at predicting flow near the wall and separation of air in the vehicle wind-tunnel experiments. In addition, Rashidi *et al.* [17] stated that using this scaled-down method in the simulation preserves how aerodynamics behaves in full scale.

The drag coefficient (Cd) values in the literature prove that high-speed trains can have a Cd in the range of 0.15 to 0.25, compared to buses that have a Cd of up to 0.8, which is proven by several authors [4], [5]. The data from the pressure and velocity contours in the simulations is similar to the results reported by Xuan *et al.* [1] and proves the reliability of the chosen CFD methodology. To conclude, the study results indicate that streamlined trains have better aerodynamics since they experience less drag and more beneficial airflow. Streamlined vehicles bring about the same results, as confirmed in scientific journals, proving how crucial a sensible shape is for enhancing a car's performance, saving energy, and providing stability.

4. Conclusions

Within this study, two Computational Fluid Dynamics (CFD) models were used to examine the aerodynamics of a streamlined high-speed train and a blunt-shaped bus in situations in which the inlet velocity was set at 10 m/s, 20 m/s, or 30 m/s. The purpose of this study was to review and measure the performance of the two models regarding boundary layer growth, the position of flow separation, the formation of the wake, pressure distribution on their surfaces, and aerodynamic effectiveness.

The simulation results clearly demonstrate that body shape significantly influences external flow behavior. The streamlined geometry of the train promotes thin, attached boundary layers, delayed flow separation, and narrow, symmetric wake formation, even at higher velocities. These characteristics result in lower pressure drag and drag coefficient values, confirming the train's superior aerodynamic efficiency. In a way, the distinctive shape of the bus leads to early flow separation because of its flat back and sharp lines. For that reason, the boundary region becomes thicker, big recirculation zones develop, and the wakes grow large and unstable when the velocity increases. The bus's high drag pressure and coefficient readings in every test showed it was not very aerodynamic and used more fuel.

Additionally, the surface pressure analysis revealed smoother pressure recovery on the train body and steep pressure drops on the bus, further highlighting the aerodynamic disadvantages of blunt shapes. The use of turbulent kinetic energy contours and velocity plots effectively visualized the wake and flow behavior behind both geometries. A grid independence test was also successfully conducted to ensure solution accuracy. The final mesh configurations provided an optimal balance between computational cost and resolution quality, confirming the robustness of the numerical approach.

Overall, the study validates the aerodynamic advantages of streamlined designs and emphasizes the importance of body shaping in reducing drag and improving flow control. These findings align well with published data and reinforce the role of CFD as a powerful tool for aerodynamic evaluation in vehicle design.

Acknowledgement

This research was supported by Universiti Tun Hussein Onn Malaysia (UTHM) through Tier 1 (Q901).

Conflict of Interest

There is no conflict of interests regarding the publication of the paper.

Author Contribution

The authors confirm their contribution to the paper, as follows: ***study conception and design:*** *Muhammad Afif Rifaie Aziz, Ishkrizat Taib;* ***data collection:*** *Muhammad Afif Rifaie Aziz;* ***analysis and interpretation of results:*** *Muhammad Afif Rifaie Aziz, Ishkrizat Taib;* ***draft manuscript preparation:*** *Muhammad Afif Rifaie Aziz, Ishkrizat Taib. All authors reviewed the results and approved the final version of the manuscript.*

References

[1] Tran Duy Duc, Duc Pham Xuan, and Vinh Nguyen Duy (2023) Aerodynamics simulation of prototype car based on CFD technology, Research Square, 1-13. https://doi.org/10.21203/rs.3.rs-3280734/v1

[2] Kshitij Bhandari, Prabin Shakya, and Krishna Prasad Shrestha (2020). Aerodynamics simulation of public bus using CFD to reduce drag and fuel consumption. International Journal of Modern Engineering Research, 10(7), 5-17.

[3] Setyadi, Pratomo, Rani Anggrainy, Yusuf Aji Widiyanto, Petra Safira, Indrianto Dicky Ismawan, and Anardratama Muhammad Owen (2024). Aerodynamic analysis of Si Jayaraya: A CFD approach to energy-efficient vehicle design, EVERGREEN Joint Journal of Novel Carbon Resource Science & Green Asia Strategy, 11(3), 2618-2623. https://doi.org/10.5109/7236901

[4] Chenyu Zhang (2024). Exploring the influence of vehicle body designs on aerodynamic drag, International Conference on Automation, Mechanical Control and Computational Engineering (AMCCE), 120, 376-383, https://doi.org/10.54097/wxzrzs08

[5] Soheila Abdolahipour (2024) review on flow separation control: effects of excitation frequency and momentum coefficient, Frontiers in Mechanical Engineering, 10, 1-23, https://doi.org/10.3389/fmech.2024.1380675

[6] Carlos Fernandez, Siti Shofiah, and Ardi Azhar Nampira (2025). The effect of aerodynamic design on fuel efficiency in commercial vehicles, Journal of Moeslim Research Technik 2(2), 87-95. https://doi.org/10.70177/technik.v2i2.1936

[7] J. Abinesh and J. Arunkumar (2014) CFD analysis of aerodynamic drag reduction and improve fuel economy International Journal of Mechanical Engineering and Robotics Research, 3(4), 430-440.

[8] Muhammad Syafiq Shaiful Anuar, Saad Kariem Shater, and Azwan Sapit (2024). Aerodynamic study of high-speed train's drag coefficient by computational fluid dynamics, Journal of Complex Flow, 6(1), 16-22.

[9] Md. Rezaul Karim Sikder and Mohammad Zoynal Abedin (2023) Numerical analysis of drag reduction using aerodynamic designs in a passenger bus, American Journal of Mechanical and Industrial Engineering, 8(4), 90-98. https://doi.org/10.11648/j.ajmie.20230804.11

[10] H. Abdul-Rahman, H. Moria, and Mohammad Rasidi Mohammad Rasani (2021) Aerodynamic study of three cars in tandem using computational fluid dynamics, Journal of Mechanical Engineering and Sciences, 15(3), 8228-8240, https://doi.org/10.15282/15.3.2021.02.0646

[11] Sunil K Arolla and Olivier Desjardins (2015), Transport modeling of sedimenting particles in a turbulent pipe flow using Euler-Lagrange large eddy simulation, International Journal of Multiphase Flow, 75, 1-11, https://doi.org/10.1016/j.ijmultiphaseflow.2015.04.010

[12] Sidi Mohammed Yousfi and Khaled Aliane (2021) Turbulent flow around obstacles: simulation and study with variable roughness, International Journal Heat and Technology, 39(5), 1659-1666, https://doi.org/10.18280/ijht.390530

[13] Sandeep Sadashiv Kore, Manoj Kumar Chaudhary, Adhikrao Sarjerao Patil, and Vijay Dilip Kolate (2023) Computational study and enhancement of heat transfer rate by using inserts introduced in a heat exchanger. Journal of Advanced Research in Fluid Mechanics and Thermal Sciences, 103(1), 16-29. https://doi.org/10.37934/arfmts.103.1.1629

[14] Beny Halfina, Muhammad Muhammad, Andik Dwi Kurniawan, Khoerul Anwar, Guino Verma, Jean Mario Valentino, Irfan Ansori, and Barep Luhur Widodo (2006). Numerical study of aerodynamics drag and flow characteristics of the high-speed train head design, ARPN Journal of Engineering and Applied Science, 19(6), 323-331.

[15] Annur Adilia Maisarah Mat, Ishkrizat Taib, Muharis Mahbubi, Wan Nur Aina Afiqah Wan Jefri, Wee Hock Teor, and Bukhari Mansoor (2025). Analysis of aerodynamics on surface of the car with turbulence models, Semarak Journal of Thermal Fluid Engineering, 4(1), 35-51. https://doi.org/10.37934/sjotfe.4.1.3551a

[16] Khurram Hameed Mughal, Salman Abubakar Bugvi, Muhammad Fawad Jamil, Basim Tamoor Baig, Taha Ahmad, Muhammad Irfan, Abdul Ahad Ashraf, and Ali Abdullah Gondal (2022). Enhancement of aerodynamic performance of high speed train through nose profile design: A computational fluid dynamics approach, Jurnal Kejuruteraan, 34(6), 1237-1250. https://doi.org/10.17576/jkukm-2022-34(6)-24

[17] Mohammad Mehdi Rashidi, Alireza Hajipour, Tian Li, Z. Yang, and Qiliang Li (2019). A review of recent studies on simulations for flow around high-speed trains. Journal of Applied and Computational Mechanics, 5(2), 311-333. https://doi.org/10.22055/JACM.2018.25495.1272

[18] Mohammad Arafat, Izuan Amin Ishak, Muhammad Aidil Safwan Abdul Aziz, Andrew Wee Shong Soh, Woei Ting Tiong, Nur Rasyidah Roziman, Nur Amiza Mohd Hairul, Muhammad Aslam Ramli, Zainal Mukhriz Ahmad Puaat, Shahrizal Hafiz Shahmuddin, and Razlin Abd Rashid (2024), A hybrid RANS/LES model for predicting the aerodynamics of small city vehicles, Journal of Advanced Research in Experimental Fluid Mechanics and Heat Transfer, 17(1), 1-13, https://doi.org/10.37934/arefmht.17.1.113

[19] Rutuja Ravindra Kapote (2023) Aerodynamic Drag reduction of heavy vehicle using Computational Fluid dynamics (CFD), Available at SSRN 4736909, 1-12. https://dx.doi.org/10.2139/ssrn.4736909

[20] Repalli Satya Venkat Narayan Murty, Pranav Pabsetti, Jai Bhoje, and Harish Rajan (2023). CFD simulation on aerodynamic performance of hyperloop vehicle. Journal of Advanced Research in Fluid Mechanics and Thermal Sciences, 102(1), 126-139. https://doi.org/10.37934/arfmts.102.1.126139